On-the-Go Mapping of Soil Mechanical Resistance Using a Linear Depth Effect Model

V. I. Adamchuk, T. J. Ingram, K. A. Sudduth, S. O. Chung

Abstract. *An instrumented blade sensor was developed to map soil mechanical resistance as well as its change with depth. The sensor has become a part of the Integrated Soil Physical Properties Mapping System (ISPPMS), which also includes an optical reflectance and a capacitor-based sensor implemented to determine spatial variability in soil organic mater and water content, respectively. The instrumented blade of the ISPPMS was validated in laboratory conditions by applying known loads. It was also tested in the field by comparing sensor-based estimates with measurements produced using a standard vertical cone penetrometer and another on-the-go sensor, the Soil Strength Profile Sensor (SSPS), consisting of five prismatic-tip horizontal penetrometers located at fixed depths. The comparison resulted in reasonable linear relationships between corresponding parameters determined using the three different methods. The coefficient of determination (r^2) for average soil mechanical resistance was 0.32 and 0.57 when ISPPMS-based estimates were compared with the standard cone penetrometer and the alternative on-the-go sensor (SSPS), respectively. Depth gradients of soil mechanical resistance obtained using cone penetrometer and ISPPMS methods were correlated with $r^2 = 0.33$. Observed differences in estimated parameters were due in part to the difficulties with obtaining data representing the same depths and in part to differences in sensor geometry and operating conditions, particularly when comparing the on-the-go sensors to the cone penetrometer. Based on its operation during Missouri field mapping, the instrumented blade proved to be a rugged and inexpensive sensor suitable for studying the spatial variability of the physical state of soils in the upper 30 cm of the profile.*

Keywords. *Precision agriculture, On-the-go soil sensors, Soil mechanical resistance.*

In many instances, spatially variable soil strength can be related to locally occurring soil compaction (Hemmat and Adamchuk, 2008). Excessive mechanical impedance can signify field conditions where increased runoff and erosion, reduced aeration, and poor development of roots can occur. On the other hand, the well-structured soils typically necessary for optimum water and nutrient holding capacity also require a sufficient level of mechanical impedance (McKyes, 1985).

Submitted for review in November 2007 as manuscript number PM 7276; approved for publication by the Power & Machinery Division of ASABE in October 2008. Presented at the 2006 ASABE Annual Meeting as Paper No. 061057.

A contribution of the University of Nebraska Agricultural Research Division, Lincoln, Nebraska. This research was supported in part by funds provided through the Hatch Act. Mention of a trade name, proprietary product, or company name is for presentation clarity and does not imply endorsement by the authors, the University of Nebraska-Lincoln, USDA-ARS, or Chungnam National University, or the exclusion of other products that may also be suitable.

The authors are **Viacheslav I. Adamchuk, ASABE Member Engineer,** Associate Professor, Department of Biological Systems Engineering, University of Nebraska, Lincoln, Nebraska; **Troy J. Ingram, ASABE Member Engineer,** Former Graduate Student, Department of Biological Systems Engineering, University of Nebraska, Lincoln, Nebraska, currently with U.S. Army Corps of Engineers; **Kenneth A. Sudduth, ASABE Fellow,** Agricultural Engineer, USDA-ARS, Columbia, Missouri; and **Sun-Ok Chung, ASABE Member Engineer,** Full-Time Instructor, Department of Bioindustrial Machinery Engineering, Chungnam National University, Daejeon, Korea. **Corresponding author:** Viacheslav I. Adamchuk, Department of Biological Systems Engineering, 203 Chase Hall, University of Nebraska, Lincoln, NE 68583-0726; phone: 402-472-8431; fax: 402-472-6338; e-mail: vadamchuk2@unl.edu.

Traditionally, penetration resistance is measured using a standardized cone penetrometer (*ASABE Standards*, 2006a). A cone penetrometer consists of a rod with a 30° cone-shaped tip attached to a load measuring device. While the cone is inserted vertically at a constant rate (3 cm s^{-1}), the insertion force is measured along with the depth of insertion. The ratio of this force to the area of the cone base is called the cone index (CI) and represents the soil penetration resistance. According to Horn and Baumgartl (2000), proper root development in many instances is observed when penetration resistance is under 2 MPa.

Because of the heterogeneous nature of soil media, cone penetrometer measurements can vary significantly even within close distances (Manor et al., 1991). Therefore, it is recommended that multiple measurements be acquired from the same location (*ASABE Standards*, 2006b). When automated (Raper et al., 1999), cone penetrometer systems can be used to effectively assess the overall degree of soil compaction in a given location. However, when it comes to mapping a production field, they become labor-demanding. To conduct dense measurements of soil mechanical resistance, various on-the-go soil sensor systems have been developed (Adamchuk et al., 2004; Hemmat and Adamchuk, 2008). These sensors have been used to measure: (1) the overall draft force (Owen et al., 1987; Mouazen et al., 2003), (2) soil mechanical resistance to instruments horizontally forced through the soil at discrete depths (Alihamsyah et al., 1990; Siefken et al., 2005; Andrade-Sánchez et al., 2007), (3) impedance to an instrument actuated vertically to vary the depth of operation (Hall and Raper, 2005), and (4) the parameters of a functional relationship between soil mechanical resistance and depth (Glancey et al., 1989; Adamchuk et al., 2001).

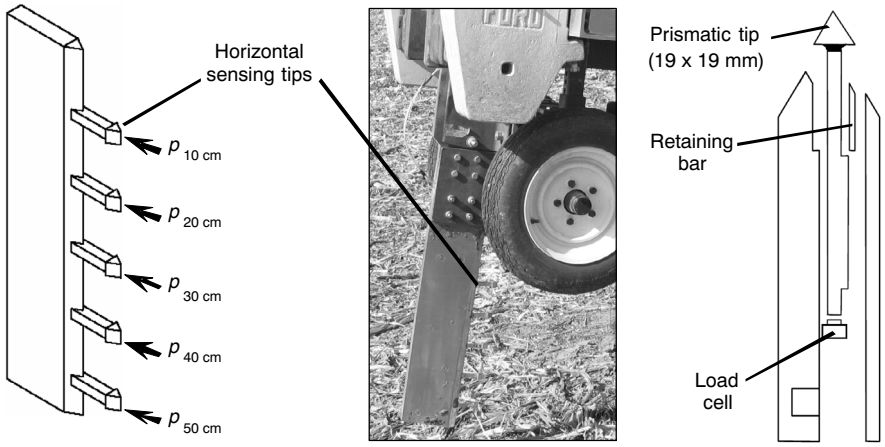

Figure 1. SSPS (left and center) and exploded top view of SSPS sensing tip configuration (right). Adapted from Chung et al. (2006).

As an example, Chung et al. (2006) developed the Soil Strength Profile Sensor (SSPS), which provided soil strength data at discrete sensing depths, nominally centered at 10, 20, 30, 40, and 50 cm below the soil surface (fig. 1). The five prismatic force-sensing tips were extended 5.1 cm ahead of the main blade to minimize the effects of soil movement by the main blade on the sensed soil strength. The force on each tip was measured by a miniaturized load cell with a 7 kN dynamic load capacity located within the main blade and in contact with the rear end of the tip shaft.

Alternatively, an Integrated Soil Physical Properties Mapping System (ISPPMS) was developed to sense several properties related to the physical state of the soil (Adamchuk and Christenson, 2007). It was comprised of an optical sensor to determine the spatial variability of soil reflectance, a capacitance sensor to estimate soil water content, and an instrumented blade to determine soil mechanical resistance at depths of 5 to 30 cm (2 to 12 in.). Each set of sensor data was georeferenced to produce corresponding maps for the follow-up decision-making process. The instrumented blade was equipped with an array of strain gauges to determine parameters of a second-order polynomial model representing the change of soil mechanical resistance with depth. However, based on field evaluation, it was concluded that in most cases the second-order coefficient was not significant, indicating a steady increase of soil mechanical resistance with depth in the top 30 cm of the soil profile. Therefore, the assumption of a linear relationship may be appropriate (Adamchuk and Christenson, 2005).

Although non-linear soil resistance profiles are often obtained when using the standard cone penetrometer method, it has been observed that cone penetrometer measurements in the top 30 cm of soil often exhibit a relatively steady increase with depth (e.g., Gorucu et al., 2006). Even if a hardpan is present between 20 and 30 cm depths, the relatively small decrease of CI below the hardpan does not significantly reduce the soil mechanical resistance applied to an instrument operated horizontally. Partially this is due to the different soil failure mode that occurs below critical depth (Hemmat and Adamchuk, 2008). On-the-go sensing of the soil profile below 30 cm requires increased drawbar power that may not be desirable in minimum tillage and no-till field operations where areas for occasional localized tillage treatments are delineated. Therefore, by maintaining a low level of soil disturbance during mapping, a linear depth effect model that can distinguish between relatively uniform soil profiles and those that exhibit a relatively high increase of soil mechanical resistance with depth within 30 cm of the soil surface is a reasonable sensing alternative (Adamchuk and Christenson, 2005).

The objectives of this project were to: (1) develop and test a prototype instrumented blade for on-the-go mapping of soil mechanical resistance using a linear depth effect model, and (2) evaluate the system's performance with respect to two other methods: the standard cone penetrometer and an on-the-go sensor capable of mapping horizontal soil mechanical resistance at discrete depths.

Materials and Methods

Instrumented Blade Development

A vertical blade equipped with a cutting edge and an array of three sets of strain gauges in a full Wheatstone bridge configuration (Dunn, 2005) was developed (fig. 2) to estimate the parameters of the following linear model representing the change of soil mechanical resistance with depth:

$$p(y) = p_0 + \delta p \cdot y \quad (1)$$

where

p = soil mechanical resistance (MPa)
p_0 = soil mechanical resistance at soil surface (MPa)
δp = depth gradient of soil mechanical resistance (MPa mm^{-1})
y = depth below soil surface (mm).

Simultaneously defined, p_0 and δp distinguish a linear model of the soil mechanical resistance profile that affects the instrumented blade measurements in the same way as the actual measured profile. Similar to Adamchuk and Christenson (2007), the new instrumented blade was a part of the ISPPMS and was developed to determine the parameters of the linear model based on the load required to move a vertical blade through the soil at a depth between 5 and 30 cm. The analyses of non-mechanical ISPPMS measurements (optical reflectance and dielectric property of soil) have been omitted from this publication.

According to the free-body diagram (fig. 2 right), linearly distributed soil mechanical resistance $p(y)$ integrated over the entire frontal area of the sensor represents the resultant soil resistance force:

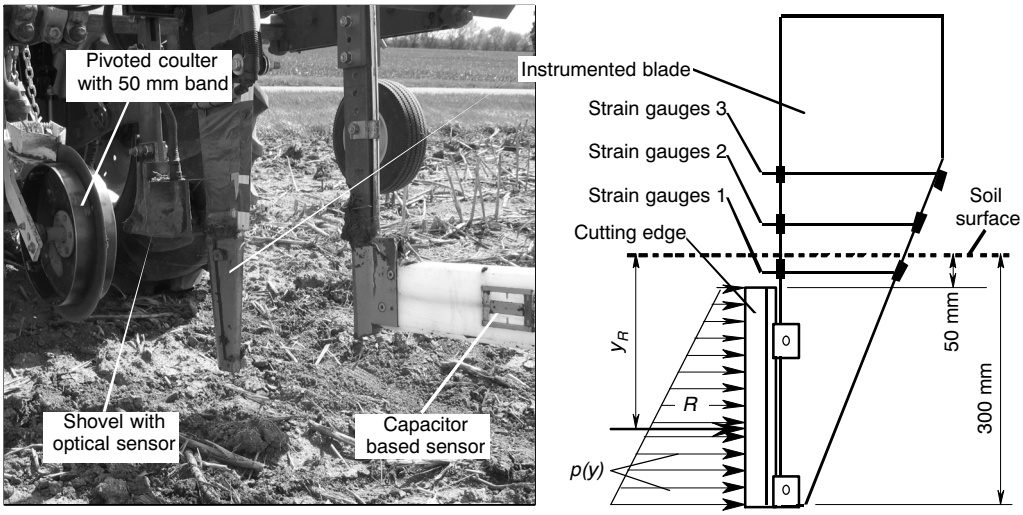

Figure 2. ISPPMS (left) and free-body diagram (right) of the ISPPMS instrumented blade.

$$R = b_e \int_{y_u}^{y_l} p(y)dy \tag{2}$$

where

R = resultant resistance force (N)
b_e = frontal width of the cutting edge (b_e = 19 mm)
y_u = depth of the upper end of the cutting edge (y_u = 50 mm)
y_l = depth of the lower end of the cutting edge (y_l = 300 mm).

This resultant force relates to the magnitude of the soil mechanical resistance. On the other hand, its vertical position with respect to the soil surface indicates the general behavior of the soil mechanical resistance profile. Thus, soil profiles with a steep increase in soil mechanical resistance with depth will produce distributions with the resultant force appearing deeper when compared to more uniform profiles. The bending moment applied to the vertical blade considered as a cantilever beam when pulled through the soil is defined as:

$$R \cdot y_R = b_e \int_{y_u}^{y_l} yp(y)dy \tag{3}$$

where y_R is the depth of the resultant resistance force R (mm).

Based on the linear depth effect model (eq. 1), both the resultant resistance force and its moment with respect to soil surface can be defined as:

$$\begin{Bmatrix} R \cdot y_R \\ R \end{Bmatrix} = \begin{bmatrix} \frac{b_e}{2}\left(y_l^2 - y_u^2\right) & \frac{b_e}{3}\left(y_l^3 - y_u^3\right) \\ b_e\left(y_l - y_u\right) & \frac{b_e}{2}\left(y_l^2 - y_u^2\right) \end{bmatrix} \begin{Bmatrix} p_0 \\ \delta p \end{Bmatrix} \tag{4}$$

Using the geometrical properties of the cutting edge, parameters p_0 and δp can be defined as:

$$\begin{Bmatrix} p_0 \\ \delta p \end{Bmatrix} = \begin{bmatrix} -6.83 \cdot 10^{-6} & 1.42 \cdot 10^{-3} \\ 3.84 \cdot 10^{-8} & -6.83 \cdot 10^{-6} \end{bmatrix} \begin{Bmatrix} R \cdot y_R \\ R \end{Bmatrix} \tag{5}$$

Similarly, the average soil mechanical resistance over the depth of measurement (5 to 30 cm) can be found as:

$$p_{avg} = \frac{R}{b_e\left(y_l - y_u\right)} \tag{6}$$

To define R and y_R, two strain gauge bridges attached to the blade at different heights would have been sufficient. However, a third set of gauges was installed to make the measurement system more reliable. Measurements produced by these gauges can be defined as:

$$\varepsilon_i = \frac{6 \cdot 10^6}{E \cdot b_b} \cdot \frac{\left(y_R - y_i\right)}{h_i^2} \cdot R \tag{7}$$

where

ε_i = measurement by ith set of strain gauges (μm m^{-1})
E = modulus of elasticity of the instrumented blade (for steel, $E = 2.07 \cdot 10^5$ MPa)
b_b = frontal width of the instrumented blade (b_b = 16 mm)
y_i = depth of ith set of strain gauges below soil surface (y_1 = 25 mm, y_2 = –64 mm, and y_3 = –152 mm; negative depth values indicate locations above the soil surface)
h_i = distance between opposite pairs of ith strain gauge bridge (h_1 = 82 mm, h_2 = 101 mm, and h_3 = 121 mm).

Based on the material and geometry of the instrumented blade, the strain to be measured by the strain gauges is:

$$\begin{Bmatrix} \varepsilon_1 \\ \varepsilon_2 \\ \varepsilon_3 \end{Bmatrix} = \begin{bmatrix} 2.75 \cdot 10^{-4} & -6.97 \cdot 10^{-3} \\ 1.77 \cdot 10^{-4} & 1.13 \cdot 10^{-2} \\ 1.24 \cdot 10^{-4} & 1.89 \cdot 10^{-2} \end{bmatrix} \begin{Bmatrix} R \cdot y_R \\ R \end{Bmatrix} \tag{8}$$

Averaging three redundant solutions for $R \cdot y_R$ and R resulted in:

$$\begin{Bmatrix} R \cdot y_R \\ R \end{Bmatrix} = \begin{bmatrix} 1908 & 3757 & -1535 \\ -20.5 & 0.0 & 45.3 \end{bmatrix} \begin{Bmatrix} \varepsilon_1 \\ \varepsilon_2 \\ \varepsilon_3 \end{Bmatrix} \tag{9}$$

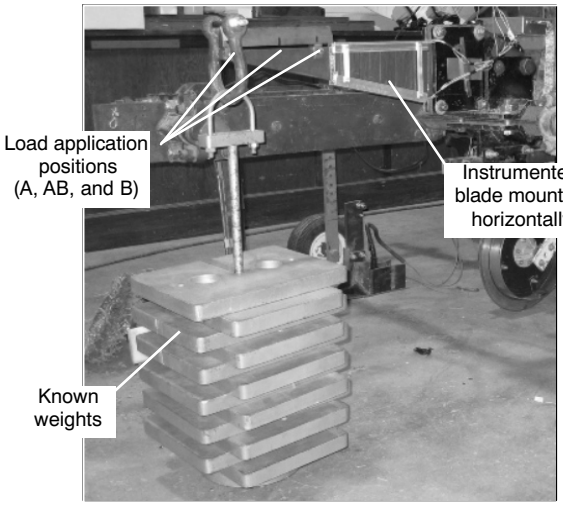

Figure 3. Laboratory evaluation of the instrumented blade.

Combining equations 5, 6, and 9 resulted in:

$$\begin{Bmatrix} p_0 \\ \delta p \\ p_{avg} \end{Bmatrix} = \begin{bmatrix} -4.22\cdot10^{-2} & -2.57\cdot10^{-2} & 7.50\cdot10^{-2} \\ 2.13\cdot10^{-4} & 1.44\cdot10^{-4} & -3.69\cdot10^{-4} \\ -4.23\cdot10^{-3} & 0 & 9.37\cdot10^{-3} \end{bmatrix} \begin{Bmatrix} \varepsilon_1 \\ \varepsilon_2 \\ \varepsilon_3 \end{Bmatrix} \quad (10)$$

Laboratory Evaluation

To validate the performance of the strain gauges, the instrumented blade was mounted horizontally (fig. 3), and different loads were applied at three points: (1) over the lower U-shaped bracket at point A (y_A = 292 mm), (2) over the upper U-shaped bracket at point B (y_B = 89 mm), and (3) 25 mm below the middle between two brackets at point AB (y_{AB} = 216 mm). In each position, the sensor was loaded and unloaded in 445 N increments, from 240 N to 2913 N. The process was repeated for each location in the same order (point A, AB, and B). Calculated (eq. 8) and measured values of strain as well as estimated (eq. 10) and actual values of loads and their application coordinates were compared.

Field Testing

Testing of the sensor was conducted in a production agriculture field located north of Centralia, in Boone County, Missouri. The field had been in a no-tillage corn-soybean rotation for more than ten years. The soils were of the Mexico series (fine, smectitic, mesic aeric Vertic Epiaqualfs) and the Adco series (fine, smectitic, mesic aeric Vertic Albaqualfs). Surface textures of these somewhat poorly drained soils ranged from silt loam to silty clay loam. The subsoil claypan horizon(s) were silty clay loam, silty clay, or clay, with 50% to 60% smectitic clay. Topsoil depth above the claypan (depth to the first Bt horizon) ranged from less than 10 cm to greater than 100 cm (Sudduth et al., 2003). The area of the field was approximately 13.4 ha.

In addition to the ISPPMS sensor, two other methods were used to measure soil mechanical resistance in this field, the Soil Strength Profile Sensor (SSPS) and a standard cone penetrometer (fig. 4). These other sensors were utilized to examine the data that were collected with the ISPPMS. The SSPS (Chung et al., 2006) was chosen because it, like the instrumented blade, runs horizontally, unlike the cone penetrometer, which takes measurements in the vertical direction. All the measurements were conducted within two days during which no precipitation occurred. Averages (and standard deviations) of gravimetric water content at the time of sampling were 0.22 (0.05), 0.27 (0.06), and 0.25 (0.05) g g^{-1} for 10, 20, and 30 cm depths, respectively.

When operating in the field, the two systems were each run at a speed of approximately 4 km h^{-1}. Previous research had shown that traveling up to this speed would not significantly affect measurements from on-the-go sensors (Siefken et al., 2005; Chung et al., 2008). The transects were made at an angle of about 45° with respect to the existing crop rows. To allow completion of on-the-go field mapping within one day, the distance between the transects was set at 10 m for the ISPPMS and 20 m for the SSPS. To avoid the soil disturbance and wheel tracks from the ISPPMS operation, SSPS transects were made in the middle between every alternate pair of

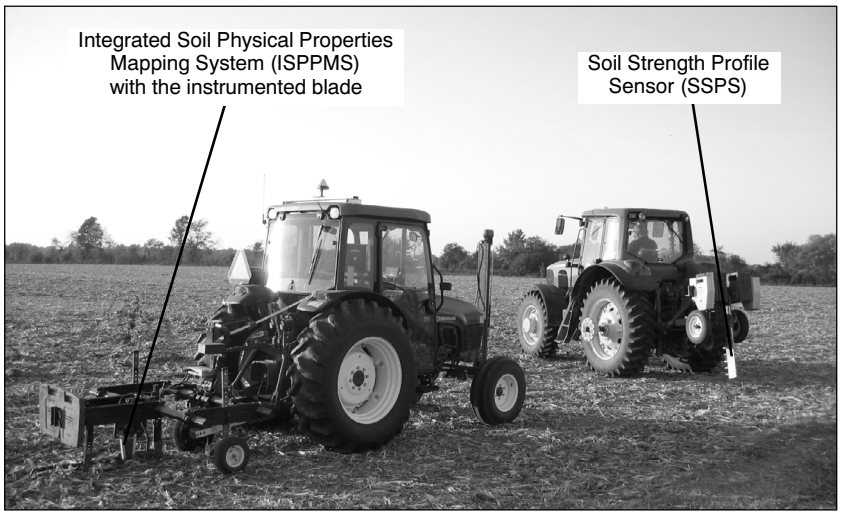

Figure 4. The two mapping systems operating in a Missouri field.

neighboring ISPPMS transects. ISPPMS data were recorded at 0.5 Hz, and the SSPS data were recorded at 1 Hz. Extraneous data points such as stops and turnarounds were filtered out. Then, 5-point (10 s) smoothing was applied to the ISPPMS data, and 9-point (9 s) smoothing was applied to the SSPS data. This difference in the averaging time period was required so that the average would be centered on the original measurement in both cases.

Cone penetrometer measurements were taken in 80 different locations (50 m square grid and an additional 19 directed points). These directed points were identified based on knowledge of field soil conditions to ensure that cone penetrometer measurements were obtained in field areas where on-the-go sensor outputs were not fluctuating. At every location, CI profiles were taken using five standard large (323 mm^2 base) cone penetrometers mounted on a single frame, similar to the device described by Raper et al. (1999). These measurements were duplicated so there were a total of ten discrete CI profile measurements at each location. These ten profiles were averaged to provide a better representation of the change in CI with depth at each location. To compare with CI profiles and with each other, the SSPS and ISPPMS measurements obtained within 15 m from the centers of the cone penetrometer measurement locations were averaged and associated with those locations.

Five different estimates provided by each measurement method were compared. These included: average soil mechanical resistance (p_{avg}), soil mechanical resistance gradient (δp), and values at three discrete depths ($p_{10\,cm}$, $p_{20\,cm}$, and $p_{30\,cm}$). Cone penetrometer measurements were recorded using 5 mm depth increments. Therefore, discrete $p_{10\,cm}$, $p_{20\,cm}$, and $p_{30\,cm}$ values were calculated by averaging CI measurements over 7.5 to 12.5 cm, 17.5 to 22.5 cm, and 27.5 to 32.5 cm depth intervals, respectively. The discrete-depth SSPS and cone penetrometer measurements were compared with $p(y)$ values calculated using p_0 and δp parameters estimated based on ISPPMS measurements, and equations 1 and 10. Thus, the ISPPMS $p(y)$ values implicitly incorporated the linear depth effect model.

Alternatively, p_{avg} and δp calculated using equation 10 were compared with most suitable estimates based on available SSPS and cone penetrometer measurements. For the SSPS, difficulties with measurement depth control and with surface residue being caught on the 10 cm sensing tip caused the $p_{10\,cm}$ values to be suspect throughout much of the field. Therefore, p_{avg} was calculated as the average of $p_{20\,cm}$ and $p_{30\,cm}$, and δp represented the difference $p_{30\,cm} - p_{20\,cm}$ divided by the 10 cm vertical distance between the two measurements. For cone penetrometer measurements, p_{avg} was calculated as the average CI from 5 to 30 cm depth, and δp was estimated as the slope of linear regression between measured CI and depth, as illustrated in figure 5.

A simple linear regression approach was used to compare the corresponding estimates produced by the different measurement methods. Variogram analysis was used to compare spatial structure revealed by the two on-the-go sensor systems.

Results and Discussion

Based on the laboratory evaluation by applying known loads to the instrumented blade mounted horizontally, a 1:1 linear relationship ($r^2 > 0.99$) was found between the calculated and measured strain values (fig. 6), which indicated the proper operation of each set of strain gauges as well as the validity of equation 8. Any residual strain was removed by zeroing the gauge output when no load was applied. Although relatively close to a 1:1 relationship, measured strain values were found to require multiplication by 0.96, 0.98, and 1.00 (strain gauges 1, 2, and 3, respectively) to match those calculated for given point loads. When using equation 9 to estimate the point load and its location based on corrected strain gauge values, the linear correlation remained strong ($r^2 > 0.99$) following a 1:1 line (fig. 7).

Average and gradient soil mechanical resistance maps (figs. 8 and 9) illustrate similarities in spatial patterns with the different measurement methods. It was noted that a few cone penetrometer measurement locations did not have corresponding SSPS measurements within the specified 15 m proximity. Basic field statistics are described in table 1. On average, the cone penetrometer produced resistance measurements with higher magnitudes and variability as compared to the on-the-go sensors. This finding was consistent with another study on a nearby field where variability in resistance was greater with a cone penetrometer than with the SSPS (Chung et al., 2008).

Pearson coefficients of correlation between the different data layers are summarized in table 2. In general, each of the

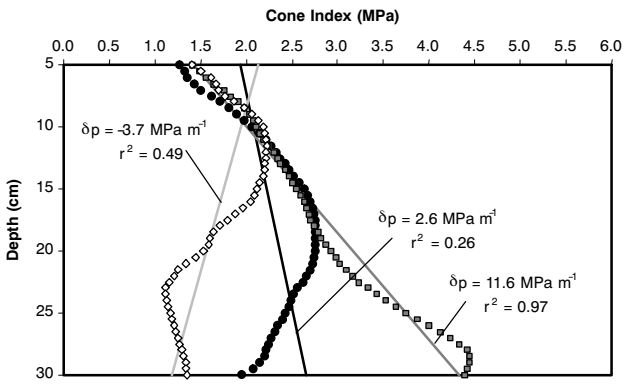

Figure 5. Three example cone penetrometer profiles from the Missouri field tested.

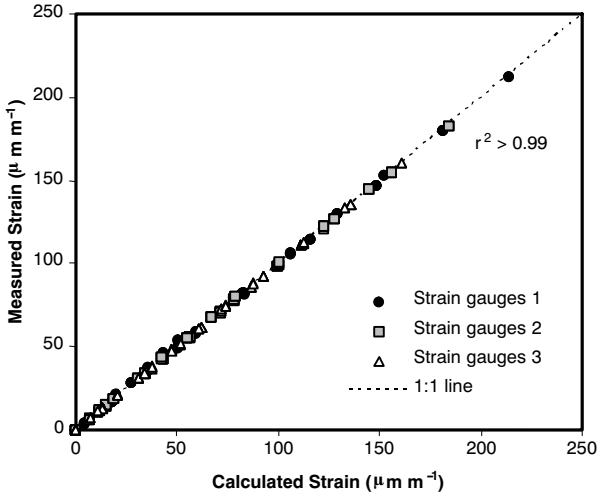

Figure 6. Relationship between calculated and measured strain values during the laboratory evaluation test.

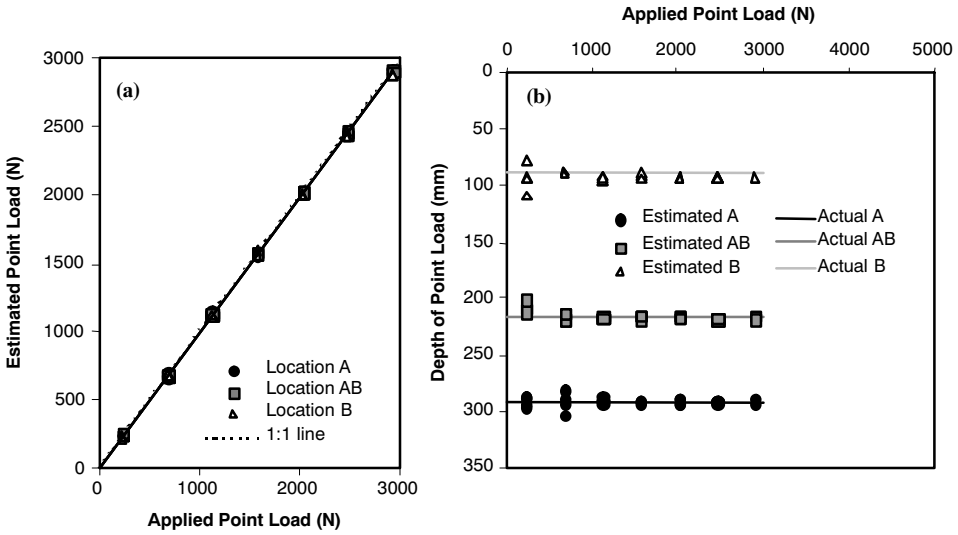

Figure 7. Relationship between (a) applied and estimated point load values and (b) estimated and actual point load locations during the laboratory evaluation test.

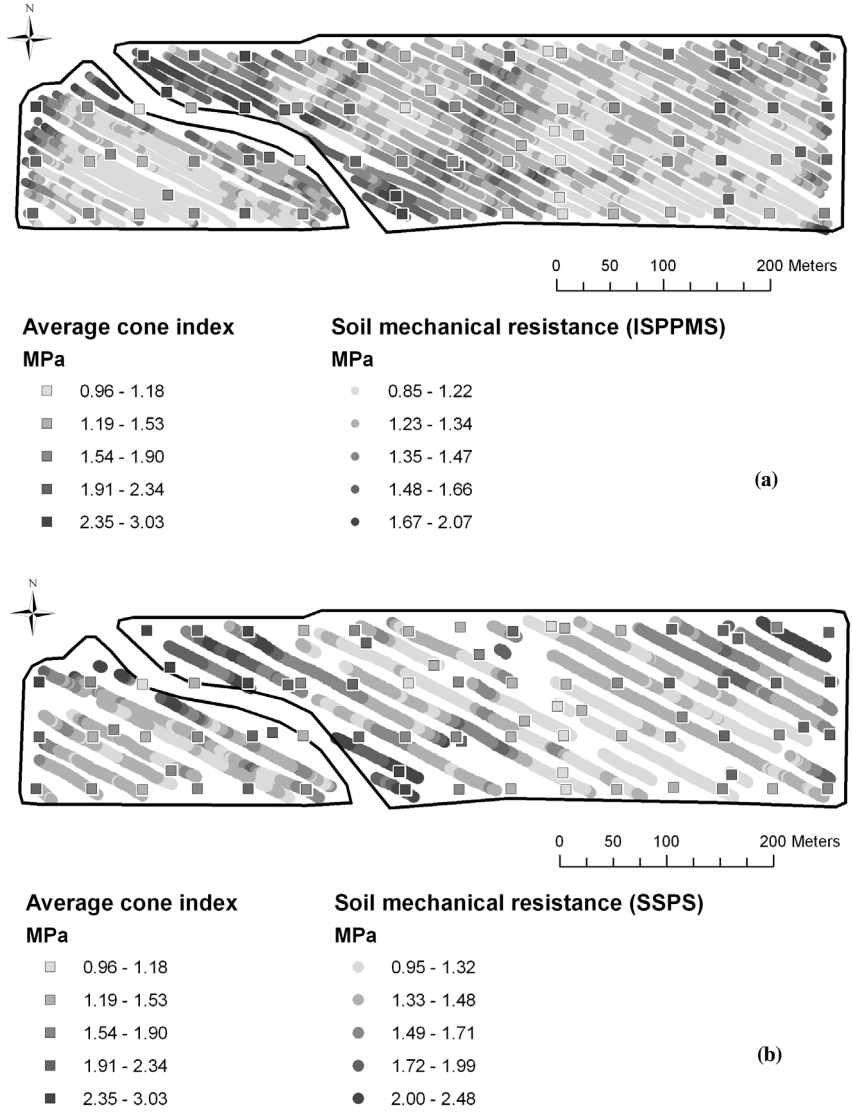

Figure 8. Maps of average soil mechanical resistance p_{avg} for (a) ISPPMS and CI, and (b) SSPS and CI.

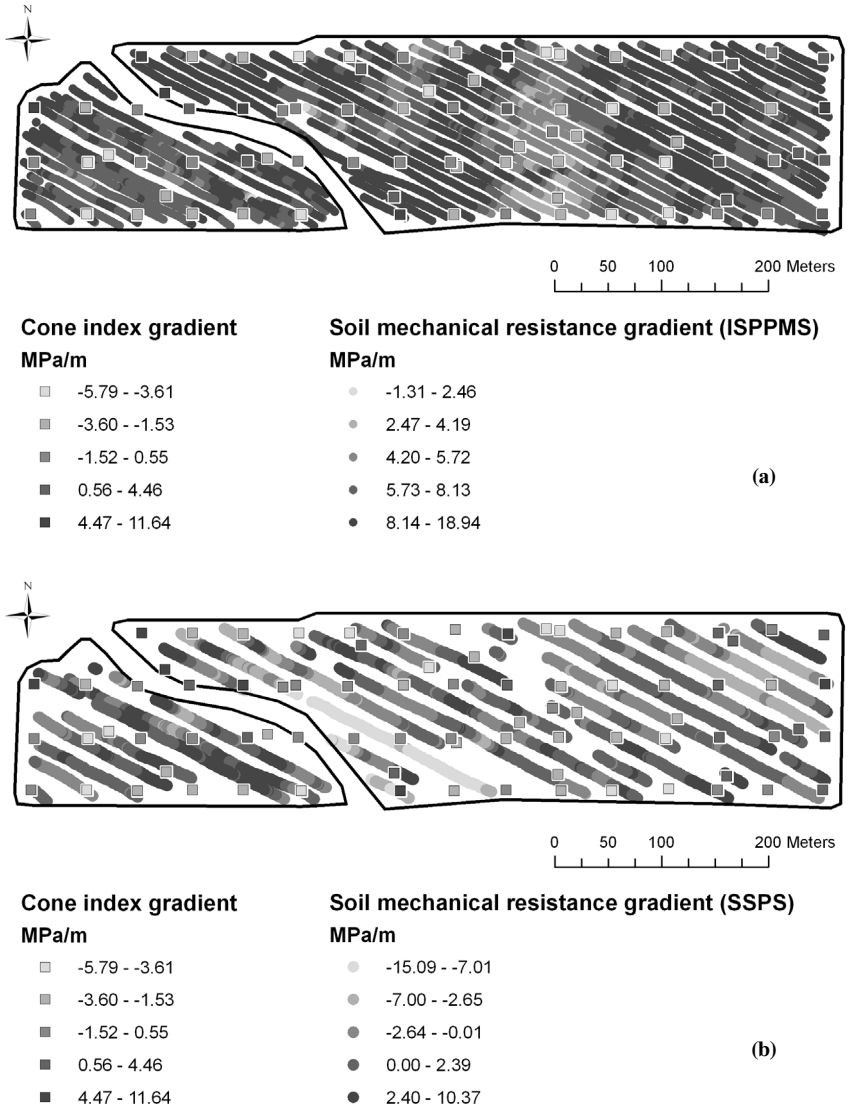

Figure 9. Maps of soil mechanical resistance gradient δ*p* for (a) ISPPMS and CI, and (b) SSPS and CI.

Table 1. Summary statistics for field data.

	p_{avg} (MPa)	δp (MPa m^{-1})	$p_{10\ cm}$ (MPa)	$p_{20\ cm}$ (MPa)	$p_{30\ cm}$ (MPa)
Cone penetrometer					
Mean	1.79	-0.54	1.91	1.81	1.63
Standard deviation	0.46	3.34	0.40	0.60	0.70
No. of measurements	80	80	80	80	80
ISPPMS					
Mean	1.34	4.50	0.99	1.44	1.89
Standard deviation	0.15	1.97	0.13	0.18	0.35
No. of measurements	5139	5139	5139	5139	5139
SSPS					
Mean	1.29	0.22	0.72	1.28	1.30
Standard deviation	0.21	2.26	0.26	0.26	0.22
No. of measurements	3654	3654	3654	3654	3654

five data layers obtained with each measurement method was significantly correlated ($\alpha = 0.05$) with some of the other data layers. However, the analysis was focused on comparison of data layers corresponding to the same physical quantities defined for the different mapping methods, shown in bold text in table 2.

Based on the comparison of values of soil mechanical resistance measured or predicted at three discrete depths (fig. 10), the 10 cm depth SSPS data ($p_{10\ cm}$) were not correlated with the corresponding cone penetrometer measurements and ISPPMS estimates. There was a negative correlation between the cone penetrometer and the ISPPMS estimates (a possible artifact of the linear depth effect model). Positive correlations were observed when comparing the $p_{20\ cm}$ and $p_{30\ cm}$ estimates. The coefficients of determination (r^2) were 0.38 and 0.47 when comparing ISPPMS with the cone penetrometer method, 0.33 and 0.35 when comparing the SSPS with the cone penetrometer method, and >0.5 when comparing the two on-the-go sensing methods. It should also be noted that neither the SSPS nor the standard cone penetrometer indicated a substantial difference in the magnitude of soil mechanical resistance between these two depths. In contrast, the magnitude of the discrete-depth soil mechanical resistance predicted from ISPPMS measurements using equations 1 and 10 varied substantially with depth.

Through further comparison of the generalized characteristics of soil mechanical resistance profiles (fig. 11), it was noted that p_{avg} had similar magnitudes for both on-the-go

Table 2. Pearson correlation coefficients between measured and calculated strength parameters from field tests.

	Cone Penetrometer					ISPPMS					SSPS				
	p_{avg}	δp	$p_{10\ cm}$	$p_{20\ cm}$	$p_{30\ cm}$	p_{avg}	δp	$p_{10\ cm}$	$p_{20\ cm}$	$p_{30\ cm}$	p_{avg}	δp	$p_{10\ cm}$	$p_{20\ cm}$	$p_{30\ cm}$
Cone Penetrometer															
p_{avg}	1.00														
δp	0.65	1.00													
$p_{10\ cm}$	0.76	NS[a]	1.00												
$p_{20\ cm}$	0.96	0.70	0.63	1.00											
$p_{30\ cm}$	0.82	0.87	0.40	0.76	1.00										
ISPPMS															
p_{avg}	**0.57**[b]	0.54	0.32	0.54	0.61	1.00									
δp	0.76	**0.58**	0.51	0.74	0.68	0.80	1.00								
$p_{10\ cm}$	-0.58	-0.31	**-0.46**	-0.58	-0.39	NS	-0.69	1.00							
$p_{20\ cm}$	0.65	0.57	0.39	**0.62**	0.65	0.98	0.90	-0.30	1.00						
$p_{30\ cm}$	0.73	0.59	0.47	0.71	**0.68**	0.91	0.98	-0.54	0.97	1.00					
SSPS															
p_{avg}	**0.68**	0.48	0.46	0.63	0.62	**0.76**	0.76	-0.35	0.79	0.79	1.00				
δp	-0.31	**NS**	-0.29	-0.26	NS	-0.31	**-0.28**	NS	-0.31	-0.30	-0.45	1.00			
$p_{10\ cm}$	NS	NS	**NS**	NS	NS	NS	NS	**NS**	NS	NS	0.27	NS	1.00		
$p_{20\ cm}$	0.64	0.42	0.46	**0.59**	0.57	0.71	0.70	-0.31	**0.73**	0.73	0.95	-0.71	0.28	1.00	
$p_{30\ cm}$	0.60	0.47	0.37	0.57	**0.57**	0.69	0.70	-0.34	0.72	**0.73**	0.89	NS	NS	0.70	1.00

[a] NS indicates non-significant correlation ($\alpha = 0.05$).
[b] **Bold** numbers indicate comparison between same parameters determined using different mapping methods.

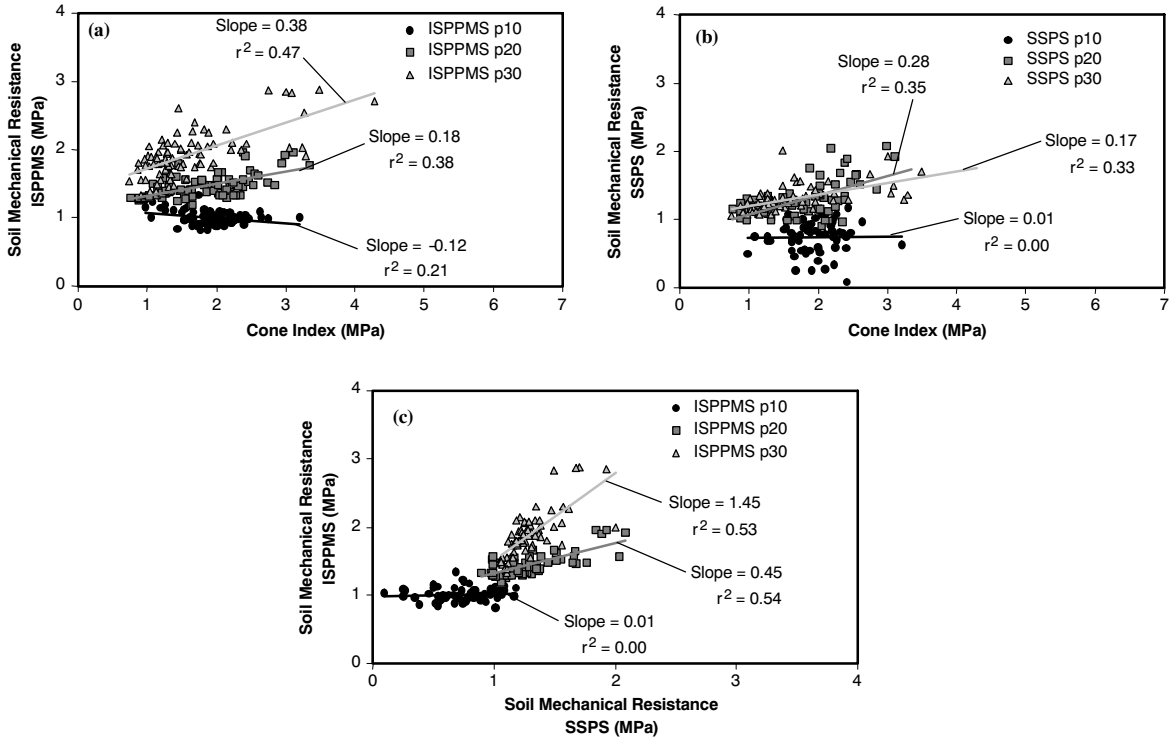

Figure 10. Relationships between discrete-depth soil mechanical resistance ($p_{10\ cm}$, $p_{20\ cm}$, and $p_{30\ cm}$) estimated using different measurement methods: (a) ISPPMS vs. CI, (b) SSPS vs. CI, and (c) ISPPMS vs. SSPS.

sensors ($r^2 = 0.57$). However, both systems produced smaller values when compared with the cone penetrometer measurements. The correlation between the SSPS and cone penetrometer estimates for p_{avg} was stronger than between the ISPPMS and cone penetrometer estimates ($r^2 = 0.46$ vs. 0.32). The gradient soil mechanical resistance (δp) determined using the SSPS measurement was negligible (between -5 and 5 MPa m^{-1}) and did not correlate with corresponding values determined using either the ISPPMS or the cone penetrometer, while a positive relationship ($r^2 = 0.33$) was found between the ISPPMS and cone penetrometer data. Comparisons of the soil mechanical resistance gradient calculated from the SSPS data to the other two sensors were not successful because the unreliable 10 cm SSPS data did not allow quantifying a soil mechanical resistance gradient compatible with the ISPPMS instrumented blade, and because there was relatively little change in soil mechanical resistance between 20 and 30 cm.

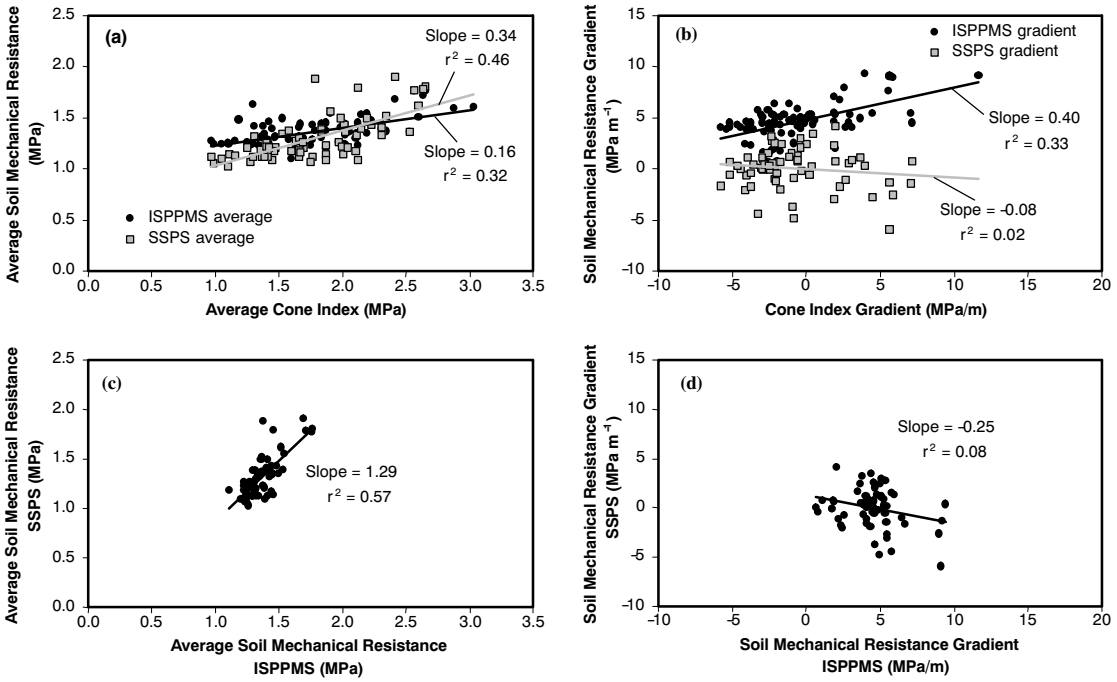

Figure 11. Relationships between average soil mechanical resistance (p_{avg}) and its gradient (δp) estimated using different measurement methods: (a, b) on-the-go sensors vs. CI, and (c, d) SSPS vs. ISPPMS.

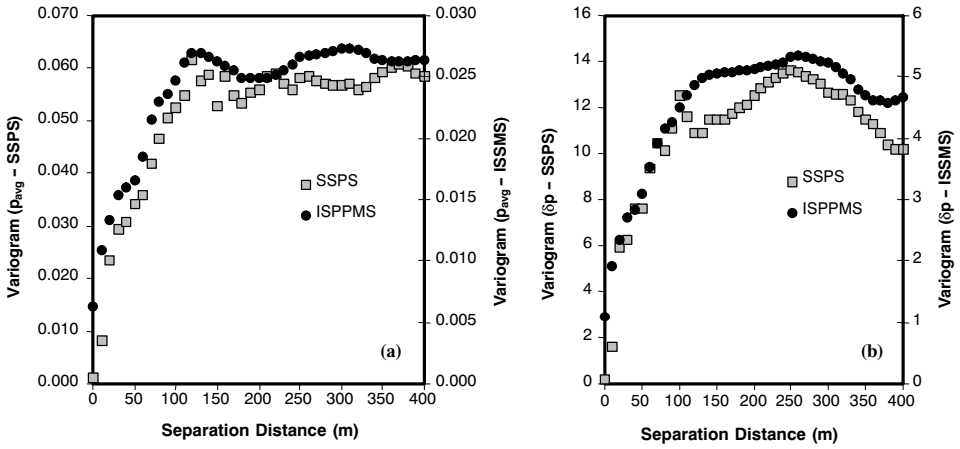

Figure 12. Variograms of (a) average soil mechanical resistance p_{avg} and (b) soil mechanical resistance gradient δp for maps obtained using SSPS and ISPPMS.

Although imperfect, a positive correlation between average soil mechanical resistance estimates produced using the two on-the-go sensors indicated that both systems were able to similarly identify field areas with variable soil strength. This was further supported through the analysis of variograms indicating very similar spatial structure (fig. 12). For both sensors, the range of spatial dependence was found to be around 130 m for both p_{avg} and δp, which suggests that linear dimensions of areas with relatively low and high measurements were similar.

Several possible reasons for the lack of close agreement were identified. The mismatch between corresponding estimates obtained using the three different measurement methods could be caused by the spatial variability of soil mechanical resistance within the 15 m radius area around each cone penetrometer location. Also, the presence of crop residue and other inconsistencies on the field surface caused depth control of both on-the-go systems to be somewhat unreliable, resulting in operation at variable depths. Furthermore, models (e.g., Chung and Sudduth, 2006) and field observations indicate that the different soil failure mechanisms generated by the different geometries and operating parameters can affect the relationship between sensor data. In particular, the lower agreement between penetrometer data and on-the-go sensor data may be at least partially explained by the geometry, operating speed, operating direction (vertical vs. horizontal), and soil failure mode differences between the sensors. A better agreement between the SSPS and ISPPMS was due to more similar operating conditions (i.e., horizontal operation at similar speeds).

Despite their differences, both on-the-go systems were capable of producing high-density (270 and 380 measurements ha^{-1}) soil maps. Integrated in nature (averaged across several crop rows), on-the-go measurements were capable of identifying the general (large-scale) field variability of soil mechanical resistance. Obtaining such information using the

cone penetrometer method would have been an extremely tedious process. The discrete-depth resistance data obtained on a relatively coarse depth resolution with the SSPS directly provided five (four, discounting the unreliable 10 cm depth) layers of data that could be used to make management decisions. Although correlated with each other, average soil mechanical resistance and its gradient, as provided by the ISPPMS, represent two different data layers that can be used to distinguish separate characteristics of the landscape (e.g., strong versus soft and uniform versus variable soil profiles). It is obvious that average soil mechanical resistance can be used to identify potentially compacted field sites.

Although the soil mechanical resistance gradient provided by the ISPPMS represented soil strength changes with depth reasonably well for these Midwestern U.S. soils, its agronomic value is yet to be evaluated through follow-up research. In different conditions where maximum compaction occurs deeper in the soil profile (e.g., Coastal Plains soils of the Southeastern U.S.), it might be necessary to increase the depth of mapping and/or return to a more complex model of the soil profile. Based on the analysis in this article, it appears that spatially variable soil productivity potential may have a similar or even greater degree of dependency on the way soil strength changes with depth as on the overall magnitude of soil mechanical resistance.

Conclusions

An instrumented blade for mapping soil mechanical resistance using a linear depth effect model was developed and tested in both the laboratory and the field. The blade was a part of a previously developed ISPPMS. Based on laboratory evaluation, strain gauges showed proper operation, and thus analytically derived relationships between forces and strain values were used. During field testing, two different on-the-go soil sensing systems were compared. The two systems were run in the same field and at the same time to reduce possible variations in field conditions. The instrumented blade for the ISPPMS determined the parameters of the linear depth effect model. The other system (SSPS) used five horizontal prismatic tips at discrete depths. The correlations that were found between the ISPPMS and SSPS on-the-go sensor systems and the standard cone penetrometer were marginal (r^2 = 0.32 to 0.46, respectively, for average soil mechanical resistance estimates), while r^2 = 0.57 for the relationship between average soil mechanical resistance measured using the two on-the-go soil sensing systems. Generally, maps produced using the two sensors revealed the same structure, as shown using variogram analysis. Some of the differences were due in part to difficulties in obtaining data at the same depth and field locations along with differences in sensor geometry and operating conditions. This was especially true when comparisons were made between the on-the-go sensors and the cone penetrometer. Depth gradients of soil mechanical resistance obtained using the soil cone penetrometer and the ISPPMS methods were correlated with r^2 = 0.33. However, the agronomic value of this measurement in the top 30 cm of the soil profile has yet to be determined.

References

Adamchuk, V. I., and P. T. Christenson. 2005. An integrated system for mapping soil physical properties on-the-go: The mechanical sensing component. In *Precision Agriculture: Papers from the Sixth European Conference on Precision Agriculture*, 449-456. J. Stafford, ed. Wageningen, The Netherlands: Wageningen Academic.

Adamchuk, V. I., and P. T. Christenson. 2007. An instrumented blade system for mapping soil mechanical resistance represented as a second-order polynomial. *Soil Tillage and Research* 95(1): 76-83.

Adamchuk, V. I., M. T. Morgan, and H. Sumali. 2001. Mapping of spatial and vertical variation of soil mechanical resistance using a linear pressure model. ASAE Paper No. 011019. St. Joseph, Mich.: ASAE.

Adamchuk, V. I., J. W. Hummel, M. T. Morgan, and S. K. Upadhyaya. 2004. On-the-go soil sensors for precision agriculture. *Computers and Electronics in Agric.* 44(1): 71-91.

Alihamsyah, T., E. G. Humphries, and C. G. Bowers. 1990. A technique for horizontal measurement of soil mechanical impedance. *Trans. ASAE* 33(1): 73-77.

Andrade-Sánchez, P., S. K. Upadhyaya, and B. M. Jenkins. 2007. Development, construction, and field evaluation of a soil compaction profile sensor. *Trans. ASABE* 50(3): 719-725.

ASABE Standards. 2006a. S313.3: Soil cone penetrometer. St. Joseph, Mich.: ASABE.

ASABE Standards. 2006b. EP542: Procedures for using and reporting data obtained with the soil cone penetrometer. St. Joseph, Mich.: ASABE.

Chung, S. O., and K. A. Sudduth. 2006. Soil failure models for vertically operating and horizontally operating strength sensors. *Trans. ASABE* 49(4): 851-863.

Chung, S. O., K. A. Sudduth, and J. W. Hummel. 2006. Design and validation of an on-the-go soil strength profile sensor. *Trans. ASABE* 49(1): 5-14.

Chung, S. O., K. A. Sudduth, C. Plouffe, and N. R. Kitchen. 2008. Soil bin and field tests of an on-the-go soil strength profile sensor. *Trans. ASABE* 51(1): 5-18.

Dunn, P. F. 2005. *Measurement and Data Analysis for Engineering and Science*. New York, N.Y.: McGraw-Hill Higher Education.

Glancey, J. L., S. K. Upadhyaya, W. J. Chancellor, and J. W. Rumsey. 1989. An instrumented chisel for the study of soil tillage dynamics. *Soil and Tillage Res.* 14(1): 1-24.

Gorucu, S., A. Khalilian, Y. J. Han, R. B. Dodd, and B. R. Smith. 2006. An algorithm to determine the optimum tillage depth from soil penetrometer data in Coastal Plain soils. *Applied Eng. in Agric.* 22(5): 625-631.

Hall, H. E., and R. L. Raper. 2005. Development and conceptual evaluation of an on-the-go soil strength measurement system. *Trans. ASAE* 48(2): 469-477.

Hemmat, A., and V. I. Adamchuk. 2008. Sensor systems for measuring soil compaction: Review and analysis. *Computers and Electronics in Agric.* 63(2): 89-103

Horn, R., and T. Baumgartl. 2000. Dynamic properties of soils. In *Handbook of Soil Science*, A19-A51. M. E. Sumner, ed. Boca Raton, Fla.: CRC Press.

Manor, G., R. L. Clark, D. E. Radcliffe, and G. W. Langdale. 1991. Soil cone index variability under fixed traffic tillage systems. *Trans. ASAE* 34(5): 1952-1956.

McKyes, E. 1985. Soil physical properties. In *Soil Cutting and Tillage*, 105-123. New York, N.Y.: Elsevier Science.

Mouazen, A. M., H. Ramon, and J. De Baerdemaeker. 2003. Modelling compaction from on-line measurement of soil properties and sensor draught. *Precision Agric.* 4(2): 203-212.

Owen, G. T., H. Drummond, L. Cobb, and R. J. Godwin. 1987. An instrumentation system for deep tillage research. *Trans. ASAE* 30(6): 1578-1582.

Raper, R. L., B. H. Washington, and J. D. Jarrell. 1999. A tractor-mounted multiple-probe soil cone penetrometer. *Applied Eng. in Agric.* 15(4): 287-290.

Siefken, R. J., V. I. Adamchuk, D. E. Eisenhauer, and L. L. Bashford. 2005. Mapping soil mechanical resistance with a multiple blade system. *Applied Eng. in Agric.* 21(1): 15-23.

Sudduth, K. A., N. R. Kitchen, G. A. Bollero, D. G. Bullock, and W. J. Wiebold. 2003. Comparison of electromagnetic induction and direct sensing of soil electrical conductivity. *Agronomy J.* 95(3): 472-482.